Superconductor-based Quantum-Dot Light-emitting Diodes (SQ-LED) : Role of Cooper-pairs to Generate Entangled Photon Pairs

Ikuo SUEMUNE[1,2]*, Tatsushi AKAZAKI[2,3], Kazunori TANAKA[2,4], Masafumi JO[1], Katsuhiro UESUGI[2,5], Michiaki ENDO[1], Hidekazu KUMANO[1,2], Eiichi HANAMURA[6], Hideaki TAKAYANAGI[2,3,7], Masamichi YAMANISHI[2,5], and Hirofumi KAN[2,5]

[1]Reseach Institute for Electronic Science, Hokkaido University, Sapporo 001-0021, Japan
[2]Japan Science and Technology Corporation (CREST), Kawaguchi, Saitama 332-0012, Japan
[3]NTT Basic Research Laboratory, Wakamiya, Morinosato, Atsugi 243-0198, Japan
[4]Central Laboratory, Hamamatsu Photonics, Hiraguchi, Hamamatsu 434-8601, Japan
[5]Faculty of Engineering, Muroran Institute of Technology, Mizumotocho, Muroran 050-8585, Japan
[6]Faculty of Photonics Science, Chitose Institute of Science and Technology, Bibi, Chitose 066-8655, Japan
[7]Department of Applied Physics, Tokyo University of Science, Tokyo 162-8601, Japan

Abstract

Realization of solid-state photon sources which are capable of on-demand generation of entangled single photon pair at a time is highly desired for quantum information processing and communication. A new method to generate entangled single photon pair at a time is proposed employing Cooper-pair-related radiative recombination in a quantum dot (QD). Cooper pairs are bosons and the control of their number states is not easy. The Pauli's exclusion principle on quasi-particles in a discrete state of a QD will regulate the number state of the generated photon pairs in this scheme. The fundamental heterostructures for constructing superconductor-based quantum-dot light-emitting diodes (SQ-LED) and the fundamental operation conditions of SQ-LED will be discussed. The experimental studies on Cooper-pair injection into the related semiconductor structures will be also discussed.

*E-mail address: isuemune@es.hokudai.ac.jp

1. Introduction

Quantum information networks are expected to offer methods for future high-speed and highly secure communications.[1] "Qubits" are the main information processing units and their storage, processing, and transportation are the basis in such information networks. Several kinds of qubits have been proposed for the processing qubits, and superconducting qubits are regarded to be one of the major research objectives because of their expandability to large-scale circuits.[2-4] Transportation of qubits will best fit with optical-fiber communication networks, and photon qubits and their applications to quantum cryptography has been actively studied.[5] However the technological basis to connect the superconducting qubits and photon qubits is missing at present because of the different historical background in the developments of the two research fields.

Concerning photon qubits, on-demand generation of entangled photon pairs is expected to explore new paradigm in communication systems such as quantum teleportations.[6] Generation of entangled photon pairs has been achieved with the parametric down conversion (PDC).[7] High degree of entanglement has been confirmed with this method.[8] However the PDC is based on excitations of nonlinear media with lasers, and therefore generated photon pairs follow the Poisson statistics. This results in random number states of the generated photon pairs and also random intervals of the generation of photon pairs. This makes it difficult to realize the on-demand photon-pair generations and purely single photon-pair generation at a time, and this limits the application of the PDC method to practical entangled photon–pair sources.

Concerning solid-state photon sources single-photon generations have been reported with single pairs of quantum states in semiconductor quantum dots (QDs), which result in exciton emissions.[9] Higher excitations of QDs result in additional biexciton emissions, and strong correlations between the biexciton emissions and the subsequent exciton emissions have been observed.[10-13] However it has been difficult to confirm quantum entanglement of the generated biexciton and exciton photon pairs in spite of tremendous trials world-wide. The main factor to prevent the quantum entanglement has been the energy splitting of the intermediate exciton states,[14] which makes the polarizations of the biexciton emissions distinguishable. The splitting of the exciton states in QDs stems from the in-plane anisotropy of QDs,[15] which originates from crystallographic surface anisotropy of semiconductor surfaces, and the resultant electron-hole exchange interactions.[14] Very recently generation of entangled photon pairs with the biexciton-exciton cascade recombination scheme was reported with a proposal to cancel the exciton energy splitting,[16] but the degree of entanglement was still low and has to be improved further.[17]

The biexciton-exciton cascade recombination processes also have the essential problem to generate ideal indistinguishable photon pairs. Because the lifetimes of the biexciton and exciton recombination are generally different, the complete overlap of the two wave forms in the time scale will be difficult. The cascade emission processes also result in the time difference between the biexciton and exciton emissions and the spin flip of the intermediate exciton states may take place during the time interval. This will induce the decoherence between the two photon states. This is detrimental for the photon qubit operations.

In this paper, a new method to generate entangled single photon pair at a time is proposed and discussed. Either electron or hole Cooper pairs are injected into a semiconductor QD, and the strong correlation of electron-electron or hole-hole in the respective Cooper pairs is expected to make it possible to recombine simultaneously into photon pairs in the QD. Cooper pairs are bosons and therefore the direct control of the number states of the generated photon pairs will not be possible. The condition to generate single photon pair at a time will be clarified. The relation to the conventional biexciton-exciton cascade emission processes and how to discriminate from this process will be discussed.

2. Main Issues in Biexciton-Exciton Cascade Emission Processes in Quantum Dots

2.1 Energy Splitting of Exciton States

Observation of strong correlations of photon pairs has been reported with the biexciton-exciton cascade recombinations in semiconductor QDs.[10-13] In isotropic QDs the bright heavy-hole exciton state (X) is spin-degenerate, and the biexciton recombination takes place either in right-circularly polarized (σ^+) or left-circularly polarized (σ^-) with the photon energy of E_{xx}, which is doubly degenerate as shown in Fig. 1(a). This is followed, respectively, by the left-circularly polarized (σ^-) or right-circularly polarized (σ^+) exciton emission with the photon energy of E_x. This cascade process is described by the following equation:

$$\Psi_{XX,X} = \frac{1}{\sqrt{2}}\left(\left| E_{XX},\sigma^+ \right\rangle_{XX} \left| E_X,\sigma^- \right\rangle_X + \left| E_{XX},\sigma^- \right\rangle_{XX} \left| E_X,\sigma^+ \right\rangle_X \right), \quad (1)$$

where the first term and the second term are indistinguishable. This represents the entangled biexciton-exciton photon-pair generations.

However energy splitting of biexciton and exciton emissions from QDs prepared on zincblende (001) surface is frequently observed, which are linearly polarized along the [110] and [1-10] crystal orientations.[14] This is originated from crystallographic anisotropy of the QD structures due to the different growth mode in the [110] and [1-10] directions. Under this circumstance, the electron-hole spin exchange interaction results in a splitting of the exciton states and the bright exciton states with the angular momentum M=±1 are split into the linearly polarized $|+1\rangle+|-1\rangle$ state and $|+1\rangle-|-1\rangle$ state as shown in Fig. 1(b). The biexciton recombination takes place either in x-polarized (π_x) or y-polarized (π_y) emission with the respective photon energy of E_{xx1} or E_{xx2}. They are followed by the x-polarized (π_x) or y-polarized (π_y) exciton emission with the respective photon energy of E_{x1} or E_{x2}. This cascade process is described by the following equation:

$$\Psi_{XX,X} = \frac{1}{\sqrt{2}}\left(\left|E_{XX_1},\pi_X\right\rangle_{XX}\left|E_{X_1},\pi_X\right\rangle_X + \left|E_{XX_2},\pi_Y\right\rangle_{XX}\left|E_{X_2},\pi_Y\right\rangle_X\right). \qquad (2)$$

In this expression, contrary to Eq. (1), the first term and the second term are distinguishable by the difference of the transition energies.

The criterion of the exciton energy splitting, which allows the quantum entanglement of the photon pairs, will be the lifetime broadening of excitons.[10)] Excitons in semiconductor QDs grown on semiconductor substrates usually exhibit the lifetimes on the order of 1 ns or less. This results in the energy broadening on the order of 2 μeV. Stevenson et al. proposed to apply a magnetic field parallel to the QD plane to reduce the exciton energy splitting.[16)] They demonstrated the quantum entanglement of the generated biexciton and exciton photon pairs by applying this method to their QDs as well as selecting QDs of which energies are close to those of the wetting layer adjacent to the QDs.[17)] The degree of entanglement is given by the quantity, tangle, which was estimated to be zero or at most 0.19[17,18)] whereas the tangle of 1 shows the complete entanglement. The purity of the quantum states is given by linear entropy, which was estimated to be ~0.9[18)] whereas the linear entropy equal to zero corresponds to the pure states. Further improvements may be possible with the refinement of the experiments in near future, but the issue of the exciton energy splitting due to the QD anisotropy still remains as the world-wide difficult problem.

2.2 Biexciton and Exciton Recombination Lifetimes

Biexciton recombination lifetimes in a QD are usually shorter than exciton recombination lifetimes because of the larger oscillator strength of biexcitons. Measurements on an InAlAs QD embedded in an AlGaAs cladding layer exemplify this and the lifetime of the biexciton lifetime was 0.55 ns and was shorter than the exciton lifetime of 1.02 ns by about half-times.[13)] This difference of the recombination lifetimes between the biexcitons and the excitons will break the indistinguishability in the photon pairs. An enhancement of the exciton oscillator strength with the aid of optical microcavities[19)] may make both lifetimes closer for generating indistinguishable photon pairs, but some elaborating efforts will be necessary for this purpose.

2.3 Spin Flip of Exciton States

The spin flip time of exciton states during the time interval after the biexciton recombination was estimated to be 2.2 ns[10)] and 3.6 ns[20)] from photon correlation measurements. These measured spin flip times are longer than the respective measured exciton lifetimes of 0.5 ns and 1.0 ns, and complete spin flip probability may not be high. However this spin flip time will reflect the scattering probability of the exciton spin state and the probability of losing the coherence between the biexciton and exciton photon pairs will not be negligible, which will be detrimental for the photon qubit operations.

3. New Scheme to Generate Single Entangled Photon Pair via Cooper-Pair Singlet States

3.1 Role of Cooper Pairs

In comparison to the PDC of the exciting photons via nonlinear optical medium,[7] simultaneous generations of photon pairs through spontaneous recombination of electrons and holes in semiconductors are not easy due to various scattering and relaxation probabilities. A unique proposal by one of the authors (E. H.) is the use of singlet states of Cooper pairs.[21] Injection of electron Cooper pairs and hole Cooper pairs into the same direct-band-gap medium via the proximity effect[22] is expected to induce spontaneous recombination of electron- and hole-Cooper-pairs, which eventually results in the generation of entangled photon pairs. This unique feature of the Cooper-pair recombination has the potential to provide a paradigm completely different from the biexciton-exciton cascade recombination.

The spin singlet states of the Cooper pairs have another advantage to the above-discussed spin-splitting issue of the exciton states, which originates from the QD anisotropy through the electron-hole exchange interactions.[14] As is well-known the biexciton states are also spin singlet states and are free from the electron-hole exchange interactions. The energy splitting of biexciton peaks frequently observed in photoluminescence (PL) spectra are due to the energy splitting of the exciton states which are the final states for the biexciton transitions. Therefore the optical transitions related to the Cooper pairs will be also free from the electron-hole exchange interactions as well as the issue of the exciton energy splitting.

3.2 Control of Number States

However since Cooper pairs are bosons, the control of the number states is not easy. Generation of single entangled photon pair at a time with the injection of the Cooper pairs needs some more sophisticated control. Nakamura et al. achieved the control of Cooper-pair qubit number states via a single Cooper-pair box.[23] It was based on the Coulomb blockade effect due to electron charge in electron Cooper pairs. Similar scheme based on the Coulomb blockade effect was previously proposed to generate single photon at a time, and the photon emitter was called as “turnstile device”.[24] The main principle was to inject single electrons and single holes to the recombination region one-by-one with the Coulomb blockade effect and to generate single photons on demand. In this scheme, single-electron and single-hole charging energies must be large enough compared to the thermal background energy to ensure single-photon emission. Therefore this device can be operated only at ultra-low temperature such as 50 mK. This operation also needs to control the tunneling processes of both electrons and holes and the operation was not simple. The scheme of the tunnel injections of electron and hole Cooper pairs via the respective single Cooper-pair boxes to generate the single entangled photon pairs will face the similar technical problems.

3.3 Proposal of Superconductor-based Quantum-Dot Light-Emitting Diode (SQ-LED)

Based on the above consideration, a new method to control the photon-pair generation process is proposed. It is based on the combination of the boson nature of the Cooper pairs and fermion nature of quasi-particles in a QD. Number states of Quasi-particles, i.e., electrons or holes, in a single quantum state in a QD are limited by the Pauli's exclusion principle and a pair of quasi-particles will form the spin singlet state in the lowest state in a QD. This will regulate the number state of the entangled photon pairs generated by the recombination with the Cooper pairs. This scheme will be realized by changing a conventional light emitting diode (LED) with QDs active medium so that either electron or hole injection into the QDs is replaced with the respective Cooper-pair injection. The fundamental device scheme and their operations of the superconductor-based quantum-dot LED (SQ-LED) will be described in the next section.

4. Fundamental Device Structures

In the following, the case of injecting electron Cooper pairs and hole quasi-particles into a QD will be mainly treated. The other case of injecting hole Cooper pairs and electron quasi-particles into a QD will be the trivial application of what is described below.

4.1 Type-II Quantum Dots

In carrier injections into QDs, energy relaxation processes are usually accompanied to populate the discrete energy states through phonon emission processes or carrier-carrier scatterings. However the situation is completely different in the case of Cooper-pair injections, and Cooper-pairs will be collapsed with such energy relaxations. Therefore resonant injection of Cooper-pairs into QD energy states is essentially important in this case. The first device structure proposed for this purpose is based on a type-II QD shown in Fig. 2. Electron Cooper-pairs are injected into the conduction band of the QD evanescently from the n-type semiconductor adjacent to the QD. Holes are injected into the QD lowest energy level through the energy relaxation processes in the valence band from the adjacent p-type semiconductor. A pair of holes will occupy the lowest state in the QD valence band due to the Pauli's exclusion principle and hole spin singlet state will be eventually formed. The detailed study of spin flip time may be important for the complete control of the dynamic properties.[25,26] The radiative recombination of the spin singlet electron Cooper pair and the hole pair will generate a circularly polarized photon pair. In this process both the initial and final states are spin singlet, and it will be free from the electron-hole exchange interactions. Therefore this recombination process will be free from the QD anisotropy issue discussed above for the biexciton-exciton cascade recombination processes. The details of the operation conditions and the discussion on the competing recombination processes such as the biexciton recombination will be given in the next section.

The heterostructure schematically shown in Fig. 2 will be possible, for example, with the following materials system. Type-II QDs are formed with GaSb QDs grown on GaAs. The band offset at the GaSb/GaAs heterointerface is critically dependent on the strain, and the conduction and valence band offsets change, respectively, from 0.10 eV and 0.81 eV for the relaxed case to 0.64 eV and 1.03 eV for the pseudomorphic case.[27] These band offsets as well as the photon emission energy can be adjusted by adopting a GaAsSb alloy for QDs, which will reduce the excess lattice mismatch of 7.8% for the GaSb/GaAs interface. Therefore the heterostructure shown in Fig. 2 will be formed by the Ga(As)Sb QDs grown on p-GaAs and by capping with n-GaAs.

The penetration depth of the electron Cooper pairs into the n-GaAs is proportional to $n^{1/3}$,[22] where n is the electron concentration in the n-GaAs capping layer. Therefore the high electron concentration in the n-GaAs layer is necessary to extend the penetration of the Cooper pairs into the Ga(As)Sb QDs through the n-GaAs capping layer. Generally heavy n-type doping in GaAs is limited due to the small density of states in the conduction band. However, our previous trials with Se-doped GaAs and GaAsNSe demonstrated the high electron concentrations up to 2×10^{19} cm^{-3} and 1×10^{20} cm^{-3}, respectively.[28] Non-alloyed ohmic contacts to n-GaAs was also possible with the use of GaAsNSe for Au contacts. This will be beneficial to form ohmic contacts for the Cooper-pair injection from a superconductor into the n-GaAs capping layer and the preliminary results will be discussed later.

As is shown in Fig. 2, the injection of the electron Cooper pair into the QD is by the tunneling through the conduction barrier in the type-II Ga(As)Sb QDs. At this point the lower conduction-band barrier height as well as the lower QD height will be beneficial to enhance the penetration of the Cooper pairs into the QD. Therefore the higher As concentration in the Ga(As)Sb QDs will be preferable for the reduced conduction-band barrier height. Concerning the QD heights, as grown GaSb QDs showed the average dot height of ~8 nm at the growth temperature of 450°C as shown in Fig. 3. The details of the growth conditions will be reported elsewhere,[29] but the QD height can be controlled via several methods. The addition of N during the growth of GaSb QDs reduced the average height to ~5 nm as shown in Fig. 3. Further reduction was observed with a purge of the GaSb dots surface with As and N supplies and the reduced average dot height of ~1.5 nm was observed. The reduction of the dot height with the method similar to the In-flush method on InAs QDs may be also possible.[30) Overflow of the holes into the n-type GaAs capping layer can be prevented by the potential height difference shown in Fig. 2 and will be possible by growing thin p-GaAsSb layer underneath the GaSb QDs.

4.2 Type-I Quantum Dots

The resonant injection of Cooper-pairs into type-I QDs will be also possible with the scheme shown in Fig. 4. When the Cooper-pair state energy in the n-type semiconductor is resonant with the QD lowest state in the conduction band, electron Cooper pairs will be injected by the tunneling through the thin barrier. The injection of holes in the valence band and the recombination processes in the QD will be similar to the one discussed in the above section.

The heterostructure schematically shown in Fig. 4 will be exemplified with the following materials system. Type-I QDs will be formed with InAs QDs buried at an n-InP/p-InP interface. For the resonant injection of electron Cooper pairs into the lowest state of the QD in the conduction band, thin $Al_{0.48}In_{0.52}As$ barrier layer lattice matched to InP will be inserted at the n-InP/InAs interface to allow tunnel injection of the Cooper pairs and to form the QD discrete states. $Al_{0.48}In_{0.52}As$ has the barrier height of 0.24 eV against InP in the conduction band.[31)] For the resonant injection into the QD lowest state, the Cooper-pair state energy in the n-type semiconductor should be adjusted so that it is resonant with the QD lowest state. This will be more adaptable by replacing n-InP with the alloy of $Al_{0.48}In_{0.52}As$ and $Ga_{0.47}In_{0.53}As$, which has the negative potential barrier of 0.26 eV to InP in the conduction band.

The advantage of this materials system is to be able to employ non-alloyed ohmic contacts by the use of InGaAs with the In composition over 70%.[32)] The experimental results on the Cooper pair injection into this materials system will be discussed in section 6. It is also noted that the type-II QD scheme shown in Fig. 2 can be realized with the InP-based materials system just by replacing the InAs QDs with GaSb QDs in the above discussions.

5. Fundamental Operations and Competing Recombination Processes

5.1 Fundamental Operation Conditions

It will be clear from the above discussion that the control of the number state of generated photon pairs is based on the Pauli's exclusion principle for the quasi-particles of holes in the QD energy states. In conventional biexciton-exciton cascade photon-pair generations in a QD, a biexciton state is initially formed every after pulsed excitation with appropriate intensity. The biexciton recombination will generate single photon from the QD, and the population in the QD is transferred to the exciton state, which eventually generate the counterpart photon for the cascade photon-pair generation.[33,34] Therefore for realizing on-demand single-photon-pair generations, the excitation pulse duration has to be short enough so that the QD will not be re-populated with biexcitons nor excitons. The similar operating conditions will apply to the present SQ-LED, that is, the appropriate bias level to populate the valence-band QD state with a pair of holes which occupy the lowest QD state and the short enough pulse duration not to re-populate the valence-band QD states prior to the subsequent pulsed excitation.

5.2 Photon-pair Generation Process and Superradiance Effect due to Cooper Pairs

The number state of the electron Cooper-pairs is described with the Wannier function as basis for the conduction band and is given by[21)]

$$|N\rangle_e \equiv \Psi_e(N) = A\sum_P (-1)^P P\prod_{i=1}^{N}\phi_e(\mathbf{r_i}-\mathbf{r_{i+N}}), \tag{3}$$

where $\phi_e(\mathbf{r_i}-\mathbf{r_{i+N}})$ is the envelope function of a Cooper pair multiplied with the Wannier functions $w_c(\mathbf{r}_i)$ and $w_c(\mathbf{r}_j)$, P is the permutation among the particles with the same spin components, i runs from 1 to N for the up-spin particles, i+N runs from N+1 to 2N for the down-spin particles, and A is a normalization constant.

The electric dipole operator **P** for interband transitions is written in terms of annihilation (creation) operators a_i (a_i^+) and b_i (b_i^+) of the electron in the conduction band and the hole in the valence band, respectively,

$$\mathbf{P} = \boldsymbol{\mu}\sum_{i=1}^{N} b_i^+ a_i \; + \; h.c., \tag{4}$$

where h.c. shows the Hermite conjugate. The interband transition dipole moment $\boldsymbol{\mu}$ is defined with the Wannier functions and is given by

$$\boldsymbol{\mu} = \int w_v^*(\mathbf{r}_i)\mathbf{p}_i w_c(\mathbf{r}_i)d\mathbf{r}_i, \tag{5}$$

where $\mathbf{p}_i$ is the momentum operator at a position $\mathbf{r}_i$.

The probability amplitude for the correlated two-photon emission from simultaneous annihilation of an electron Cooper pair and a spin singlet hole pair in the lowest QD state in the valence-band is described in terms of the interaction Hamiltonian, $H' = -\mathbf{E}\cdot\mathbf{P}$, and is given by[21)]

$$H'_{(2)} = \left\langle \Psi_e(N-1)\left|\sum_m \frac{H'|m\rangle\langle m|H'}{E_i - E_m}\right|\Psi_e(N)w_v(\mathbf{r}_i)w'_v(\mathbf{r}_i)\right\rangle$$

$$\cong 2\sqrt{N}\frac{|\boldsymbol{\mu}\cdot\mathbf{E}|^2}{\Delta_e}, \qquad (6)$$

where Δ_e is the half of the superconductor gap $2\Delta_e$. Since the transition probability, i.e., the oscillator strength, is proportional to $|H'_{(2)}|^2$, it is proportional to the number of the electron Cooper pairs in the active medium, i.e., in the QD. This implies a superradiance process which comes from the coherent state of N Cooper-pairs.[21] In the following, the enhancement of the oscillator strength due to the superradiance effect will be estimated for a QD active medium.

The total number of electrons, n_s, which contribute to the supercurrent is related to the critical current density, j_c, by the relation[35]

$$j_c = \frac{en_s\Delta_e}{p_F}, \qquad (7)$$

where p_F is the momentum of the quasi-particles which contribute to the supercurrent near the Fermi energy. n_s is estimated to be $8\text{x}10^{21}$ cm^{-3} in a typical superconductor such as Sn.[35] Doping levels in semiconductors are normally limited to the lower level, and the injection of Cooper pairs into n-type semiconductors will be limited by the available electron concentrations in the n-type semiconductors. The penetration depth of the Cooper pairs into n-type semiconductors is also limited by the electron concentration n in the form of $n^{1/3}$,[22] and the number of the Cooper pairs in actual devices will be space-dependent. But for the purpose of estimating the QD size dependence of the superradiance effect, the relative variation of the effective number of the Cooper pairs in a QD will be estimated under the simplified situation that the Cooper-pair number equals to n/2.

The relative dependence on the QD size was estimated and is shown in Fig. 5. The electron concentration in n-type semiconductor was set to $5\text{x}10^{18}cm^{-3}$ and a disc-like QD with the dot diameter to dot height ratio of D/H=10 was assumed. Relatively flat QD structure can be formed by such as the In-flush method.[30] The enhancement of the oscillator strength with the superradiance effect is critically dependent on the QD size, and the larger coherent volume will contribute to the larger oscillator strength. The corresponding transition energy in a GaSb QD embedded in GaAs was calculated with a simplified method discussed in Ref. 31. Since the GaSb/GaAs system forms the QD energy states in the valence band, the calculated transition energy of the lowest QD state shown in Fig. 6 reflect the valence-band QD state. The materials parameters necessary for this calculation are given in Ref. 36. The oscillator strength shown in Fig. 5 is more enhanced for the larger QD, but the critical issue is the energy separation of the lowest and second QD excited state transitions. However, the possible contribution from the transitions from the higher excited states in QDs will be spectrally filtered as is usually practiced in the observations of the biexciton-exciton cascade photon-pair emission.

5.3 Other Competing Recombination Processes

The possible recombination processes are schematically shown in Fig. 7. One Cooper pair in the conduction band and two holes in the lowest heavy-hole (HH) band are assumed. The case I is the process mainly dealt with in this paper and single photon pair will be generated simultaneously with the enhanced oscillator strength as discussed in the previous section. The photon energy of the generated photon pairs will be given by

$$\hbar\omega = E_g + E_{HH1} - 2\Delta_e, \tag{8}$$

where E_g is the energy gap of the QD under compressive strain and E_{HH1} is the confinement energy in the QD valence band.

The case II is the competing process where one of the electron Cooper pair dissolves the pairing and recombines with one of the hole pair in the HH1 state. This is accompanied with the generation of one quasi-particle above the superconducting gap of $2\Delta_e$ by absorbing acoustic phonon. In this process, the photon energy of the generated single photon is also given by Eq. (8) but additionally

$$E_{acoustic} = 2\Delta_e + \frac{\hbar^2 k_c^2}{2m_c^*},\ \hbar k_c - \hbar k_{acoustic} = 0, \tag{9}$$

need to be satisfied, where m_c^* is the effective mass of the normal electron, and k_c and $k_{acoustic}$ are the wave numbers of the normal electron and the acoustic phonon, respectively. When the operation at extremely low temperature is assumed, the acoustic phonon population will be low and this process with the absorption of acoustic phonon will be unlikely.

The case III is the competition with the conventional biexction recombinations. In this process, the two quasi-particles apparently have the energy higher than the Cooper pair by $2(2\Delta_e)$. However the formation of the biexciton states with the hole pair in the valence band will be stabilized by the exciton binding energy. Therefore the relation of the case I and the case III is critically dependent on the oscillator strengths of the respective transitions. The biexciton binding energy is usually positive and the biexciton recombination normally dominates in type-I QDs. However there exist reports of negative exciton binding energies in type-I InAs QDs.[37)] Negative biexciton binding energy has been also observed in GaN QDs under the internal electric field.[38)] In type-II QDs, negative biexciton binding energy is predicted theoretically.[39)] Under these situations with negative biexciton binding energies, the case I with the Cooper-pair-based recombination will predominate the case III with the biexciton recombination.

The case IV may take place under the low population of holes in the QD valence band.

Under the single population of the hole in the QD state, the Cooper pair may be eventually dissociated and one of them may recombine with the hole in the valence band. The other quasi-particle will be excited above the superconducting gap with the absorption of acoustic phonons similarly to the case II. Similar to the case II, the probability to absorb phonons at extremely low temperature will be low. The detailed balance of each process needs more rigorous calculations and the study is under way.

6. Experiments on Cooper-pair Injection into Semiconductors

Cooper-pair injection into semiconductors is a prerequisite to realize the generation of entangled single photon pair at a time with recombination between electron Cooper pairs and hole quasi-particles in a QD. To confirm the capability to inject Cooper pairs into semiconductors, a Nb/n-InGaAs/Nb vertical Josephson junction was prepared and was investigated on its superconducting properties.

Figure 8 shows the schematic structure of the Nb/ n-InGaAs /Nb vertical Josephson junction. The n-InGaAs heterostructure was grown by metal-organic vapor-phase epitaxy (MOVPE) on a semi-insulating (100) InP substrate. A pair of the Nb electrodes were formed on 10-nm-thick n^+-$In_{0.7}Ga_{0.3}As$ highly doped (with the electron concentration higher than $3x10^{19}cm^{-3}$) layers to obtain good ohmic contact without annealing. The critical temperature T_C of the Nb superconducting electrodes was about 7.5 K. The fabrication process is following. A Si_3N_4 passivation film was deposited on the In-rich n^+-InGaAs layer by plasma chemical vapor deposition (PCVD), and the Si_3N_4 film in the junction area was removed by reactive ion etching (RIE) using a photoresist pattern as a mask. To define Nb electrodes for the measurements, the lift-off technique was employed using a separately prepared photoresist pattern. Oxidation on the n^+-InGaAs surface was removed by Ar sputtering in a Nb evaporation chamber. After that, Nb electrodes were deposited by electron beam deposition and then lifted off. Then the InP substrate was lapped to the thickness of about 100 μm. The InP substrate in the junction area was removed selectively by wet chemical etching with an HCl-based etchant. It was followed by the formation of the Nb electrodes on the backside n^+-InGaAs layer by means of the same procedure as the front Nb electrode. The processed wafer was cleaved to form rectangular device chips with the area of 1.5mm x 1.5mm.

Figure 9 shows the current-voltage (I-V) characteristics of the Nb/ n-InGaAs /Nb vertical Josephson junction measured at 0.7 K. A critical current I_C of about 130 μA can be estimated from the current value at the corners of the I-V characteristics. This result demonstrates that the Josephson current through the 100-nm-thick n-InGaAs layer was observed and that Cooper pairs can be injected into the n-InGaAs semiconductor layer.

Similar trial to inject Cooper pairs to GaAs-based semiconductors has been done.[40] The

GaAsNSe highly n-type doped layer[28)] was employed for non-alloyed ohmic contacts for a Nb/n-GaAs/Nb lateral Josephson junction. The Nb stripe electrodes with the width of 20 μm and the electrode separation of 0.7 μm were prepared on the n-type GaAs surface with the GaAsNSe ohmic-contact layer, which was removed in the surface area separating the two Nb electrodes. The sub-harmonic-gap structure due to multiple Andreev reflection was observed at 0.5 K.[40)] The extension of this trial to confirm the Cooper-pair injection into n-GaAs layers is under study.

7. Conclusion

Present major efforts to generate entangled photon pairs from solid-state sources are focused to biexciton-exciton cascade photon-pair emissions. The major issues remaining in this research direction were clarified, and the method to solve the central issue of the exciton-state energy splitting was proposed employing Cooper-pair injection into semiconductor quantum dots. The fundamental heterostructures for constructing the proposed SQ-LED and its fundamental operation conditions were discussed. The experimental confirmation of Cooper-pair injection into the related semiconductor structure was also demonstrated.

Acknowledgements

The authors are grateful to Mr. T. Maruyama of NTT-AT for his Cooper-pair injection measurements. They also thank Dr. Y. Hayashi, Mr. S. Kimura, Mr. S. Kobayashi, Dr. Sasakura, Prof. S. Adachi, and Prof. S. Muto of Hokkaido Univ. for the related luminescence measurements, and Dr. Y. Idutsu of Hokkaido Univ. for epitaxy of the related QD structures.

References

1) M. A. Nielsen and I. L. Chuang: *Quantum Computation and Quantum Information, Cambridge University Press*, Cambridge (2000).

2) J. E. Mooij, T. P. Orlando, L. Levitov, L. Tian, C. H. van der Wal, S. Lloyd: Science **285** (1999) 1036.

3) S. Saito, M. Thorwart, H. Tanaka, M. Ueda, H. Nakano, K. Semba, and H. Takayanagi: Phys. Rev. Lett. **93** (2004) 037001.

4) T. Yamamoto, Y. A. Pashkin, O. Astafiev, Y. Nakamura, and J. S. Tsai: Nature **425** (2003) 941.

5) for example, N. Gisin, G. Ribordy, W. Tittel, and H. Zbinden: Review of Modern Physics, **74** (2002) 145.

6) D. Bouwmeester, A. Ekert, and A. Zeilinger (edited): The Physics of Quantum Information, Springer-Verlag, Berlin (2000).

7) P. G. Kwiat, K. Mattle, H. Weinfurter, A. Zeilinger, A. V. Sergienko, and Y. Shih: Phys. Rev. Lett. **75** (1995) 4337.

8) A. G. White, D. F. V. James, W. J. Munro, and P. G. Kwiat: Phys. Rev. A **65** (2002) 012301.

9) P. Michler, A. Imamoglu, M. D. Mason, P. J. Carson, G. F. Strouse, and S. K. Buratto: Nature **406** (2000) 968.

10) C. Sntori, D. Fattal, M. Pelton, G. S. Solomon, and Y. Yamamoto: Phys. Rev. B, **66** (2002) 045308.

11) S. M. Ulrich, S. Strauf, P. Michler, G. Bacher, and A. Forchel: Appl. Phys. Lett. **83** (2003) 1848.

12) I. Robert, E. Moreau, J. M. Gerard, I. Abram: J. Luminescence **94-95** (2001) 797.

13) H. Kumano, S. Kimura, M. Endo, I. Suemune, H. Sasakura, S. Adachi, S. Muto, H. Z. Song, S. Hirose, and T. Usuki: Physica E **32** (2006) 144.

14) V. D. Kulakovskii, G. Bacher, R. Weigand, T. Kummell, A. Forchel, E. Borovitskaya, K. Leonardi, and D. Hommel: Phys. Rev. Lett. **82** (1999) 1780.

15) for example, M. Arita, A. Avramescu, K. Uesugi, I. Suemune, T. Numai, H. Machida, and N. Shimoyama: Jpn. J. Appl. Phys. **36** (1997) 4097.

16) R. M. Stevenson, R. J. Young, P. Atkinson, K. Cooper, D. A. Ritchie and A. J. Shields: nature 439 (2006) 04446.

17) R. J. Young, R. M. Stevenson, P. Atkinson, K. Cooper, D. A. Ritchie, A. J. Shields: New J. of Phys. **8** (2006) 29.

18) A. Gilchrist, K. J. Resch, A. G. White: arXiv:quant-ph/0602018.

19) C. Santori, D. Fattal, J. Vuckovic, G. S. Solomon, and Y. Yamamoto: nature 410 (**2002**)

594.
20) H. Kumano, S. Kimura, M. Endo, H. Sasakura, S. Adachi, S. Muto, and I. Suemune: J. Nanoelectron. and Optoelectron. **1** (2006) 40.
21) E. Hanamura: phys. stat. sol. (b) **234** (2002) 166.
22) P. G. de Gennes: *Superconductivity of Metals and Alloys*, Westview Press, ABP, Boulder (1999).
23) Y. Nakamura, Yu. A. Pashkin, and J. S. Tsai: Nature **398**, 786-788 (1999) 786.
24) J. Kim, O. Benson, H. Kan, and Y. Yamamoto: Nature **397** (1999) 500.
25) T. Flissikowski, I. A. Akimov, A. Hundt, and F. Henneberger: Phys. Rev. B **68** (2003) 161309.
26) R. Spiegel, G. Bacher, A. Forchel, B. Jobst, D. Hommel, and G. Landwehr: Phys. Rev. B **55** (1997) 9866.
27) F. Hatami, N. N. Ledentsov, M. Grundmann, J. Boehrer, F. Heinrichsdorff, M. Beer, D. Bimberg, S. S. Ruvimov, P. Werner, U. Goesele, J. Heydenreich, U. Richter, S. V. Ivanov, B. Ya. Meltser, P. S. Kop'ev, and Zh. I. Alferov: Appl. Phys. Lett. **67** (1995) 656.
28) K. Uesugi and I. Suemune: Appl. Phys. Lett. **79** (2001) 3284.
29) K. Uesugi, M. Kurimoto, I. Suemune, M. Yamamoto, T. Uemura, H. Machida, and N. Shimoyama: Physica E **21** (2004) 727.
30) C. Paranthoen, N. Bertru, O. Dehaese, A. Le Corre, S. Loualiche, B. Lambert, and G. Patriarche: Appl. Phys. Lett. **78** (2001) 1751.
31) I. Vurgaftman, J. R. Meyer, L. R. Ram-Mohan: J. Appl. Phys. **89** (2001) 5815.
32) K. Kajiyama, Y. Mizushima, and S. Sakata: Appl. Phys. Lett. **23** (1973) 458.
33) A. Kiraz, S. Falth, C. Becher, B. Gayral, W. V. Schoenfeld, P. M. Petroff, L. Zhang, E. Hu, and A. Imamoglu: Phys. Rev. B **65** (2002) 161303.
34) Z. Yuan, B. E. Kardynal, R. M. Stevenson, A. J. Shields, C. J. Lobo, K. Cooper, N. S. Beattie, D. A. Ritchie, M. Pepper: Science **295** (2002) 102.
35) A. G. Rose-Innes and E. H. Rhoderick: *Introduction to Superconductivity*, Pergamon Press Ltd, (1978).
36) I. Suemune, G. Sasikala, H. Kumano, K. Uesugi, Y. Nabetani, T. Matsumoto, J.-T. Maeng, and T.-Y. Seong: Jpn. J. Appl. Phys. **45** (2006) L529.
37) S. Rodt, R. Heitz, A. Schliwa, R. L. Sellin, F. Guffarth, and D. Bimberg: Phys. Rev. B **68** (2003) 035331.
38) S. Kako, K. Hoshino, S. Iwamoto, S. Ishida, and Y. Arakawa: Appl. Phys. Lett. **85** (2004) 64.
39) P. Lelong, K. Suzuki, G. Bastard, H. Sakaki and Y. Arakawa: Physica E **7** (2000) 393.
40) T. Akazaki, T. Maruyama, H. Takayanagi, M. Jo, K. Uesugi, and I. Suemune: Extended

Abstracts of the 52th Spring Meeting of The Japan Society of Applied Physics and Related Societies, 24a-H-5 (2005) 254 (in Japanese).

Figure captions

Fig. 1. Biexciton(XX) and exciton(X) recombination processes. (a) Exciton is degenerate. (b)Exciton is spin-split.

Fig. 2. Cooper-pair injection scheme in type-II quantum dot for entangled photon-pair generation.

Fig. 3. Relation of dot height and dot diameter for GaSb dots grown on (001) GaAs. Dot height can be controlled by the simultaneous supply of N during growth of QD or purge of GaSb dot surface with combined As and N supplies.

Fig. 4. Cooper-pair injection scheme in type-I quantum dot for entangled photon-pair generation.

Fig. 5. Dot size dependence of the estimated oscillator strength enhancement factor due to superradiance effect. Ratio of QD diameter to height was fixed to 10 in this example.

Fig. 6. Dot size dependence of transition energy between conduction band and valence-band lowest QD state in type-II GaSb QD and energy separation of lowest to second state QD transition energies. Ratio of QD diameter to height was fixed to 10 in this example.

Fig. 7. Possible recombination processes (a) ~(d) of electron Cooper pairs injected into a QD with hole quasi-particles.

Fig. 8. Schematic structure of Nb/n-InGaAs/Nb vertical Josephson junction. (a) cross-sectional view. (b) top view.

Fig. 9. Current-voltage characteristic of Nb/n-InGaAs/Nb vertical Josephson junction measured at 0.7 K.

Fig. 1

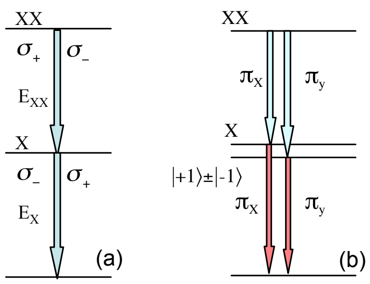

XX
σ_+
σ_-
E_{XX}
X
σ_-
σ_+
E_X
(a)
XX
π_x
π_y
X
$|+1\rangle \pm |-1\rangle$
π_x
π_y
(b)

Fig. 2

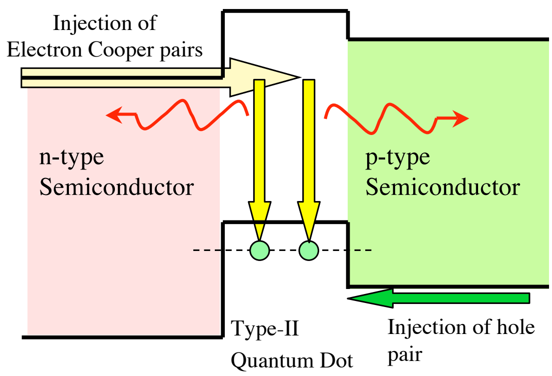

Injection of Electron Cooper pairs
n-type Semiconductor
p-type Semiconductor
Type-II Quantum Dot
Injection of hole pair

Fig. 3

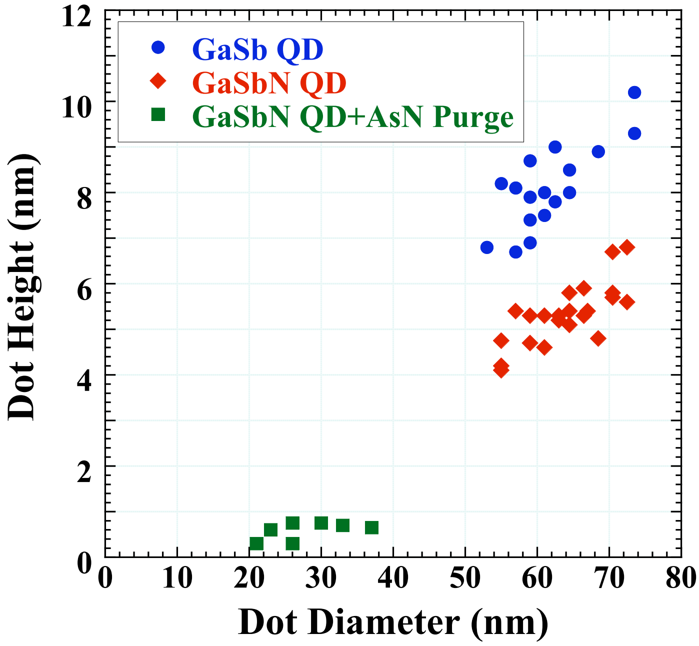

GaSb QD
GaSbN QD
GaSbN QD+AsN Purge
Dot Height (nm)
Dot Diameter (nm)
0
2
4
6
8
10
12
0
10
20
30
40
50
60
70
80

Fig. 4

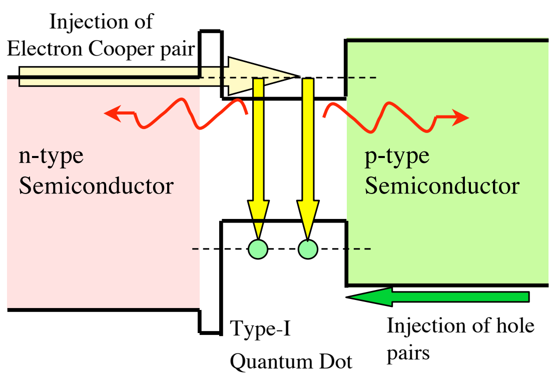

Injection of
Electron Cooper pair
n-type
Semiconductor
p-type
Semiconductor
Type-I
Quantum Dot
Injection of hole
pairs

Fig. 5

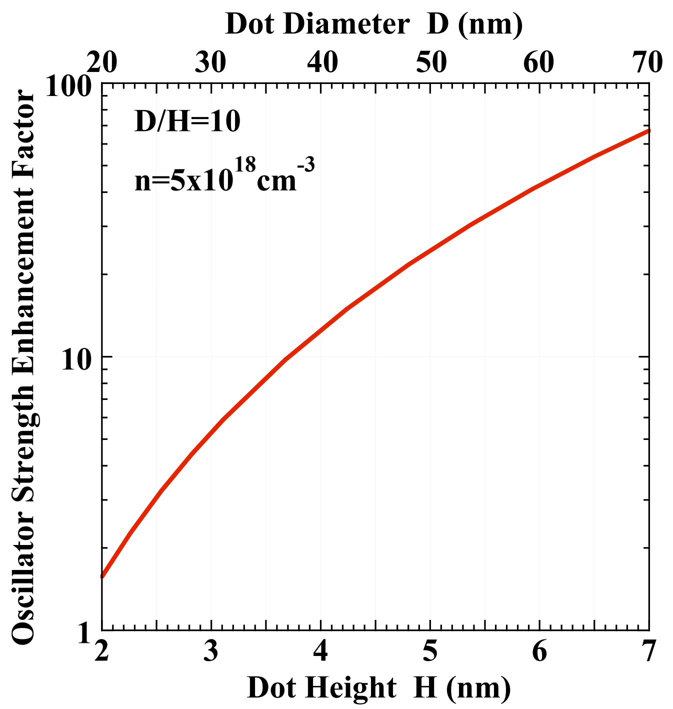
Dot Diameter D (nm)
20 30 40 50 60 70
100
10
1
D/H=10
n=5x10^18 cm^-3
Oscillator Strength Enhancement Factor
2 3 4 5 6 7
Dot Height H (nm)

Fig. 6

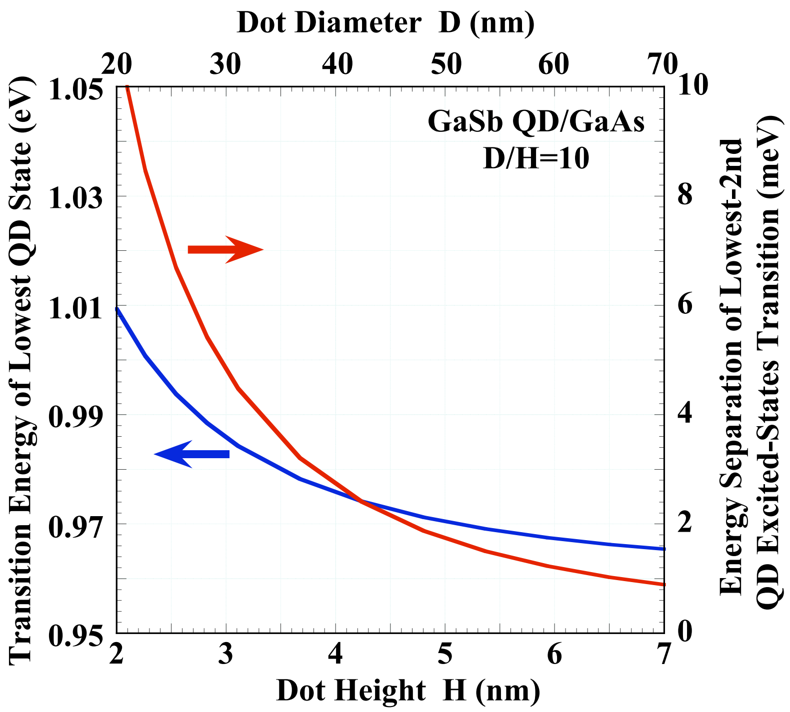
Dot Diameter D (nm)
20 30 40 50 60 70
1.05
1.03
1.01
0.99
0.97
0.95
10
8
6
4
2
0
GaSb QD/GaAs
D/H=10
Transition Energy of Lowest QD State (eV)
Energy Separation of Lowest-2nd QD Excited-States Transition (meV)
2 3 4 5 6 7
Dot Height H (nm)

Fig. 7

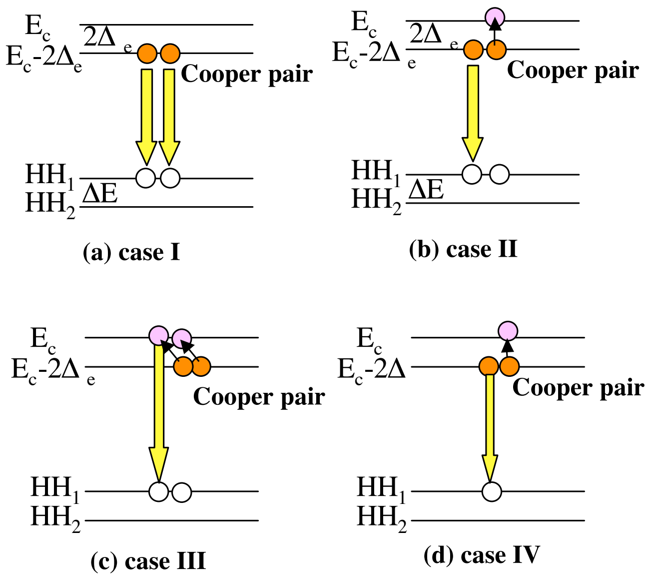

E_c
2Δ e
E_c-2Δ e
Cooper pair
HH1
ΔE
HH2
(a) case I
E_c
2Δ e
E_c-2Δ e
Cooper pair
HH1
ΔE
HH2
(b) case II
E_c
E_c-2Δ e
Cooper pair
HH1
HH2
(c) case III
E_c
E_c-2Δ
Cooper pair
HH1
HH2
(d) case IV

Fig. 8

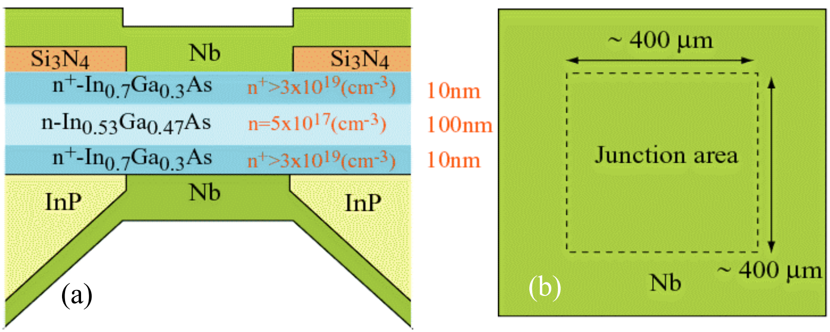

Nb
Si3N4
Si3N4
n+-In0.7Ga0.3As n+>3x10^19(cm^-3) 10nm
n-In0.53Ga0.47As n=5x10^17(cm^-3) 100nm
n+-In0.7Ga0.3As n+>3x10^19(cm^-3) 10nm
InP
Nb
InP
(a)
~ 400 µm
Junction area
~ 400 µm
(b)
Nb

Fig. 9

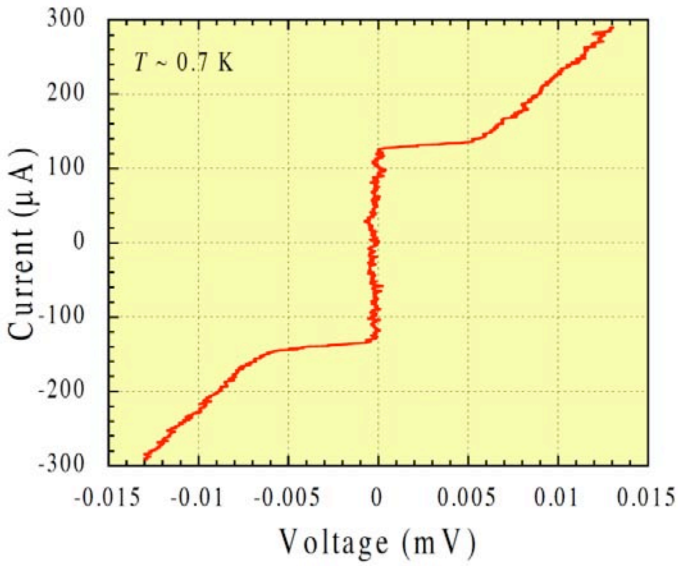

T ~ 0.7 K
300
200
100
0
-100
-200
-300
Current (μA)
-0.015
-0.01
-0.005
0
0.005
0.01
0.015
Voltage (mV)